

# Optimal Stiffener Design for Interior Sound Reduction Using a Topology Optimization Based Approach

Jianhui Luo

Hae Chang Gea

Department of Mechanical and Aerospace  
Engineering,  
Rutgers, The State University of New Jersey,  
Piscataway, NJ 08855

*A topology optimization based approach is proposed to study the optimal configuration of stiffeners for the interior sound reduction. Since our design target is aimed at reducing the low frequency noise, a coupled acoustic-structural conservative system without damping effect is considered. Modal analysis method is used to evaluate the interior sound level for this coupled system. To formulate the topology optimization problem, a recently introduced Microstructure-based Design Domain Method (MDDM) is employed. Using the MDDM, the optimal stiffener configurations problem is treated as a material distribution problem and sensitivity analysis of the coupled system is derived analytically. The norm of acoustic excitation is used as the indicator of the interior sound level. The optimal stiffener design is obtained by solving this topology optimization problem using a sequential convex approximation method. Examples of acoustic box under single frequency excitation and a band of low frequency excitations are presented and discussed.*

[DOI: 10.1115/1.1569512]

## 1 Introduction

The reduction of low frequency noise is of great interest in designing transportation vehicles because the 20-200 Hz low frequency noise has an important influence on the product satisfactory quality. In the automobile passenger compartment, the low frequency noise can be generated by engine vibration or induced by road roughness; in the aircraft cabin, the low frequency noise can be originated from engines, propellers or aerodynamic forces. Although active vibration control is a fast growing research field, passive vibration controls from structural optimization techniques are often used in practice due to their low implementation cost. Studies of noise reduction by structural modification are found in the literature. Hagiwara et al. [1] investigated the reduction of vehicle interior noise with shell thickness redistribution using the sensitivity information semi-analytically. Huff, Jr. and Bernhard [2] used a parametric shape optimization method in the reduction of the sound pressure level. Wodtke and Koopmann [3], Constants and Belegundu [4] introduced the structural modifications by placing optimally sized point masses in order to minimize the radiated sound power of vibrating structures.

In this paper, a topology optimization based approach is proposed to study the optimal configuration of stiffeners for interior sound reduction. Since our design target is aimed at reducing the low frequency noise, a coupled acoustic-structural conservative system without damping effect is considered. Modal analysis method is used to evaluate the interior sound level for this coupled system [5]. To formulate the topology optimization problem a recently introduced Microstructure-based Design Domain Method (MDDM) [6] is employed. Using the MDDM, the optimal stiffener configurations problem is treated as a material distribution problem and sensitivity analysis of the coupled system is derived analytically. The optimal stiffener design is obtained by solving this topology optimization problem using a sequential convex approximation method called Generalized Convex Approximation [7].

The remainder of the paper is organized as follows: Section 2

introduces the modal analysis approach to calculating the frequency response for the coupled acoustic-structural system; Section 3 discusses the sensitivity analysis of frequency response for this system. In Section 4, topology optimization problem is formulated and the solution procedure of identifying the optimal configurations of stiffeners for the reduction of the interior sound level is described. In Section 5, four numerical examples of an acoustic box under external excitations are presented. Conclusion remarks and future work are discussed in the final section.

## 2 Frequency Response of Coupled Systems

In this section, frequency response of coupled acoustic-structural systems is derived from the modal analysis method. Consider that a coupled acoustic-structural system consists of an enclosure surrounded by an elastic body and the elastic body is subjected to both force and displacement boundary conditions as shown in Fig. 1. Using the finite element method to discretize the coupled system yields the following equations [8]

$$\begin{bmatrix} M_{ss} & 0 \\ M_{as} & M_{aa} \end{bmatrix} \begin{Bmatrix} \ddot{u}_e \\ \ddot{p}_e \end{Bmatrix} + \begin{bmatrix} K_{ss} & K_{sa} \\ 0 & K_{aa} \end{bmatrix} \begin{Bmatrix} u_e \\ p_e \end{Bmatrix} = \begin{Bmatrix} f_s \\ 0 \end{Bmatrix} \quad (1)$$

where the upper equation refers to the structural system and the lower equation refers to the acoustic system. In these equations,  $u_e$  is the vector representing displacement components at the grid points of the structural finite element model,  $p_e$  is the vector representing sound pressures at the grid points of the acoustic finite element model.  $f_s$  represents the external forces applied to the structure, such as mechanical excitations.  $M_{ss}$  and  $K_{ss}$  are structural mass and stiffness matrices,  $M_{aa}$  and  $K_{aa}$  are acoustic mass and stiffness matrices.  $M_{as}$  and  $K_{sa}$  are acoustic-structural coupling matrices, and they have the property of  $K_{sa} = -M_{as}^T$ . The structural and acoustic equations of motion are coupled through the matrix  $M_{as}$  which transforms the structural accelerations to acoustic excitations of the interior cavity, and through the matrix  $K_{sa}$  which transforms the acoustic pressures to loads acting on the structure.

If the external force has a harmonic form of  $f_s e^{i\omega t}$ , then the structural and acoustic responses can be expressed as  $u_e e^{i\omega t}$  and

Contributed by the Technical Committee on Vibration and Sound for publication in the JOURNAL OF VIBRATION AND ACOUSTICS. Manuscript received June 1997; Revised October 2002. Associate Editor: R. L. Clark.

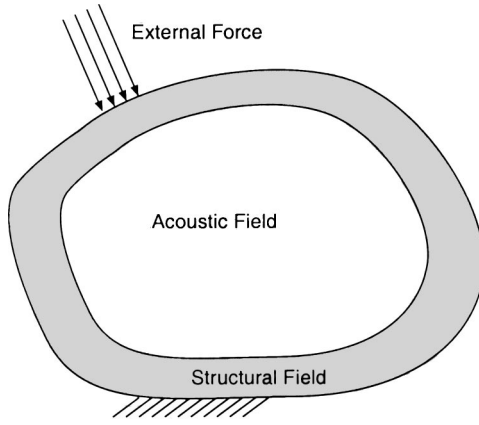


Fig. 1 A coupled acoustic-structural system

$p_e e^{i\omega t}$ , where  $\omega$  is the excitation frequency. Introducing these expressions to Eq. (1) yields the frequency response equation as

$$\begin{bmatrix} K_{ss} - \omega^2 M_{ss} & K_{sa} \\ -\omega^2 M_{as} & K_{aa} - \omega^2 M_{aa} \end{bmatrix} \begin{Bmatrix} u_e \\ p_e \end{Bmatrix} = \begin{Bmatrix} f_s \\ 0 \end{Bmatrix} \quad (2)$$

There are two different approaches to computing frequency response in Eq. (2): the direct method and the modal analysis method. The direct method is a rather straightforward approach that solves Eq. (2) directly but it is very computationally expensive. On the other hand, the modal analysis method is extremely attractive because both structural and acoustic modal density are relatively low under the low excitation frequencies. Therefore, the modal analysis method is adopted in this study.

Since the mass and stiffness matrices are unsymmetric in the coupled acoustic-structural system, the left eigenvectors are not the same as the right ones. Using the modal analysis method, the right eigenvalue problem can be formulated as

$$\begin{bmatrix} K_{ss} & K_{sa} \\ 0 & K_{aa} \end{bmatrix} \begin{Bmatrix} \Psi_s \\ \Psi_a \end{Bmatrix} = [\Lambda] \begin{bmatrix} M_{ss} & 0 \\ M_{as} & M_{aa} \end{bmatrix} \begin{Bmatrix} \Psi_s \\ \Psi_a \end{Bmatrix} \quad (3)$$

where  $\Lambda$  is the eigenvalue matrix;  $\Psi_s$  and  $\Psi_a$  are the right eigenvector matrices corresponding to the structural and acoustic fields respectively. Similarly, the left eigenvalue problem is represented as

$$\{\bar{\Psi}_s^T \quad \bar{\Psi}_a^T\} \begin{bmatrix} K_{ss} & K_{sa} \\ 0 & K_{aa} \end{bmatrix} = [\Lambda] \{\bar{\Psi}_s^T \quad \bar{\Psi}_a^T\} \begin{bmatrix} M_{ss} & 0 \\ M_{as} & M_{aa} \end{bmatrix} \quad (4)$$

where  $\bar{\Psi}_s$  and  $\bar{\Psi}_a$  denote the left eigenvector matrices of the structural and acoustic fields. The M-orthonormal condition of the coupled system is stated as follows:

$$\{\bar{\Psi}_s^T \quad \bar{\Psi}_a^T\} \begin{bmatrix} M_{ss} & 0 \\ M_{as} & M_{aa} \end{bmatrix} \begin{Bmatrix} \Psi_s \\ \Psi_a \end{Bmatrix} = [I] \quad (5)$$

For large coupled acoustic-structural systems, it is impractical to solve Eq. (3) and Eq. (4) directly because of the high computational cost. Luo and Gea [5] proposed a symmetrization approach to effectively extract eigenmodes with less computational time and storage. They also proved that the right eigenvectors and the left eigenvectors of a coupled system can be related as

$$\begin{Bmatrix} \bar{\Psi}_s \\ \bar{\Psi}_a \end{Bmatrix} = \begin{Bmatrix} \Lambda \Psi_s \\ \Psi_a \end{Bmatrix} \quad (6)$$

Suppose that the forced frequency responses are expanded by the right eigenvectors of the coupled system as

$$\begin{Bmatrix} u_e \\ p_e \end{Bmatrix} = \Psi \xi \quad (7)$$

where  $\Psi = \{\Psi_s \quad \Psi_a\}^T$  denotes the right eigenvector matrix of the coupled system,  $\xi$  is the coefficient matrix.

Inserting Eq. (7) into the governing equations of Eq. (2) and premultiplying both sides by left eigenvector matrix  $\bar{\Psi}^T = \{\bar{\Psi}_s^T \quad \bar{\Psi}_a^T\}$ , the use of M-orthonormal condition leads to

$$([\Lambda] - \omega^2 [I]) \xi = \bar{\Psi}^T \begin{Bmatrix} f_s \\ 0 \end{Bmatrix} = \bar{\Psi}_s^T f_s \quad (8)$$

Denote  $\bar{\Psi}_s^T f_s = \mathbf{p}$ , the coefficient matrix  $\xi$  can be computed in the following form

$$\xi_i = \frac{p_i}{\lambda_i - \omega^2} \quad (9)$$

where  $\xi_i$ ,  $p_i$  and  $\lambda_i$  are the  $i^{th}$  component of  $\xi$ ,  $\mathbf{p}$  and  $\Lambda$ . Combining Eq. (9) with Eq. (7), the response of the coupled acoustic-structural system is recovered.

### 3 Sensitivity Analysis of Coupled Systems

When an optimization problem is solved by mathematical programming algorithms, we must determine the effect resulting from a small perturbation in the current design on the objective and constraint functions. This is known as the sensitivity analysis. In this study, frequency response sensitivities are the derivatives of structural response and the sound pressure with respect to the structural modification design variables. With the correct frequency response sensitivity information, one can use various optimization methods to arrive at a modified structure with reduced interior sound level. The frequency response sensitivity,  $\{u'_e, p'_e\}^T$ , can be derived by differentiating Eq. (2) as

$$\begin{bmatrix} K_{ss} - \omega^2 M_{ss} & K_{sa} \\ -\omega^2 M_{as} & K_{aa} - \omega^2 M_{aa} \end{bmatrix} \begin{Bmatrix} u'_e \\ p'_e \end{Bmatrix} = - \begin{bmatrix} K'_{ss} - \omega^2 M'_{ss} & 0 \\ 0 & 0 \end{bmatrix} \begin{Bmatrix} u_c \\ p_e \end{Bmatrix} \quad (10)$$

where  $K'_{ss}$  and  $M'_{ss}$  are the derivatives of the structural stiffness and mass matrices with respect to the design variable, respectively.

If we define a pseudo load  $g_s = -[K'_{ss} - \omega^2 M'_{ss}]u_e$ , Eq. (10) can be rewritten as

$$\begin{bmatrix} K_{ss} - \omega^2 M_{ss} & K_{sa} \\ -\omega^2 M_{as} & K_{aa} - \omega^2 M_{aa} \end{bmatrix} \begin{Bmatrix} u'_e \\ p'_e \end{Bmatrix} = \begin{Bmatrix} g_s \\ 0 \end{Bmatrix} \quad (11)$$

Eq. (11) has the same form as the frequency response governing equations in Eq. (2) except the excitation force has been changed from  $f_s$  to  $g_s$ . Therefore, the solution of Eq. (11) can be obtained in the same way as shown in the previous section.

Assume response sensitivities can be decomposed as,  $\{u'_e, p'_e\}^T = \Psi \eta$  with  $\eta$  being the undetermined coefficient matrix. Put this expansion into Eq. (11) and premultiply both sides by  $\bar{\Psi}^T$ , we have

$$([\Lambda] - \omega^2 [I]) \eta = \bar{\Psi}^T \begin{Bmatrix} g_s \\ 0 \end{Bmatrix} = \bar{\Psi}_s^T g_s \quad (12)$$

Denote  $\bar{\Psi}_s^T g_s = \mathbf{q}$ , then coefficient matrix can be determined in the indices form

$$\eta_i = \frac{q_i}{\lambda_i - \omega^2} \quad (13)$$

With Eq. (13), the frequency response sensitivity,  $\{u'_e, p'_e\}$ , can be calculated easily.

### 4 Solution Procedures

In this section, the solution procedures of identifying the optimal configuration of stiffeners placement for the reduction of the interior sound level are discussed.

The overall interior sound level for the acoustic field is evaluated as

$$SPL = \frac{1}{m} \sum_{i=1}^m (10 \log_{10}[p_i/p_0]^2) \quad (14)$$

where  $p_i$  denotes the sound pressure at the  $i^{th}$  node,  $m$  is the total number of nodal points in the acoustic field,  $p_0$  is a reference pressure, normally, chosen as  $2 \times 10^{-5}$  Pa.

Although  $SPL$  is a direct indicator of sound noise, it inherits strong localized effects from individual nodal pressure. Therefore, if this function is used as the objective function in the optimization process, search algorithm will exhibit unstable oscillations and consequently have difficulty to converge. Consider the fact that the level of interior sound is fully determined by the acoustic excitation, that can be measured by the magnitude of  $-\omega^2 M_{as} u_e$  from Eq. (2) for a given excitation frequency. The minimization of the norm of  $-\omega^2 M_{as} u_e$  can lead to the reduction of SPL. Therefore, the minimization of the acoustic excitation is chosen as the objective function. In our numerical examples, iteration histories of SPL are also listed for the purpose of comparing the sound pressure level reductions from the optimization process.

When a structure is subjected to a band of frequency excitations  $[\omega_0, \omega_1]$ , the objective function can be modified as

$$\text{Minimize } \frac{1}{\omega_1 - \omega_0} \int_{\omega_0}^{\omega_1} \|-\omega^2 M_{as} u_e(\omega)\| d\omega \quad (15)$$

And, the overall interior sound level from Eq. (14) can be defined as

$$SPL = \frac{1}{\omega_1 - \omega_0} \int_{\omega_0}^{\omega_1} \left( \frac{1}{m} \sum_{i=1}^m (10 \log_{10}[p_i(\omega)/p_0]^2) \right) d\omega \quad (16)$$

Recently, the stiffener layout optimization problem is tackled by material distribution formulations, in which a given amount of “artificial” stiffener material is dispersed optimally to the base structure for the best structure performance. The material model for the combination of base material and “artificial” stiffener material is often borrowed from various theories of composite materials. This method is called the topology optimization because the topology of stiffener design is to be optimized. Diaz and Kikuchi [9] used this technique on solving stiffener layout design optimization under natural frequency and they applied the homogenization theory [10] to evaluate the material properties of the composite consisting of the base and stiffener material. In this paper, a Microstructure-based Design Domain Method (MDDM) introduced by Gea [6] is applied to model the add-on stiffener. In the MDDM, material is treated as a “composite” consisting of matrix and spherical inclusion materials. The effective material properties of the  $i$ th element is expressed in the form

$$\kappa^{(i)} = \kappa_0 \left( 1 + \frac{c_1^{(i)}(\kappa_1 - \kappa_0)}{(1 - c_1^{(i)})\alpha_0(\kappa_1 - \kappa_0) + \kappa_0} \right) \quad (17)$$

$$\mu^{(i)} = \mu_0 \left( 1 + \frac{c_1^{(i)}(\mu_1 - \mu_0)}{(1 - c_1^{(i)})\beta_0(\mu_1 - \mu_0) + \mu_0} \right) \quad (18)$$

with

$$\alpha_0 = \frac{1}{3} \frac{1 + \nu_0}{1 - \nu_0} \quad (19)$$

$$\beta_0 = \frac{2}{15} \frac{4 - 5\nu_0}{1 - \nu_0} \quad (20)$$

where subscripts 0 and 1 represent matrix and inclusion materials;  $\kappa$  and  $\mu$  denote the bulk modulus and the shear modulus.  $\nu_0$  is Poisson's ratio of the matrix, and  $c_1^{(i)}$  is the volume fraction of the inclusion material in the  $i$ th element. Using this model, the vol-

ume fraction,  $c_1^{(i)}$ , is treated as the design variables in the stiffener topology optimization formulation: as  $c_1^{(i)} = 0$  no stiffener is required and  $c_1^{(i)} = 1$  stiffener exists. Using these relation,  $K'_{ss}$  and  $M'_{ss}$  under the pseudo load can be directly calculated.

Generally, the total allowable weight of the structure is considered as a design constraint that cannot exceed a prescribed amount. The optimization problem of minimizing acoustic excitation is stated as,

$$\text{Minimize } \|-\omega^2 M_{as} u_e\| \quad (21)$$

$$\text{Subject To: } \sum_{i=1}^N \rho v_i (1 + c_1^{(i)}) \leq \bar{W} \quad (22)$$

where  $\rho$  denotes the material density,  $v_i$  is the volume of  $i$ th element,  $c_1^{(i)}$  is the design variable as described previously,  $N$  is the number of elements, and  $\bar{W}$  is the upper limit of total weight.

In order to search for the optimal stiffener topology, the number of design variables is related to the number of finite elements used in the structural model. Therefore, the optimizer used here must be very efficient in handling a large number of design variables. In this paper, the Generalized Convex Approximation (GCA) method introduced by Chickermane and Gea [7] is used to formulate and solve the topology optimization problem. In the GCA, functions are approximated as the sum of a series of separable functions of the design variables as

$$f(x) \cong f(x^k) - \sum_i^n b_i(x_i^k - d_i)^{r_i} + \sum_i^n b_i(x_i - d_i)^{r_i} \quad (23)$$

where  $b_i$ ,  $d_i$  and  $r_i$  are a set of approximation parameters to be determined, and  $f(x^k)$  is the value of the original function at the  $k$ th design. Function values and first order sensitivity information from the current and previous design is utilized to determine the values of the approximation parameters. The approximation problem is solved iteratively using mathematical programming to generate the next design. This process continues until a satisfactory design is reached.

## 5 Numerical Examples

Optimal stiffener designs of an aluminum alloy (1100-H14) box using the proposed topology optimization based method are presented in this section. The aluminum box of  $30 \text{ cm} \times 40 \text{ cm} \times 50 \text{ cm}$  is fixed at four bottom corners and under various external excitations. The aluminum plate has thickness 0.2 cm, Poisson's ratio 0.33, Young's modulus  $6.9 \times 10^{10}$  Pa, density  $2.7 \times 10^3 \text{ kg/m}^3$  and the box without any stiffeners weights 5.076 Kg. The “artificial” stiffen material has the same density as the base material but with 100 times higher strength in order to simulate the strong rigidity effect produced by stiffeners. The upper weight limit of the add-on “artificial” stiffen material is set to be 10% of the total base weight. That gives the total allowable weight of the whole structure be 5.5836 Kg. In the initial design, the add-on “artificial” stiffen material is uniformly distributed to the box in order to produce an unbiased starting point. From the analyses of the initial design, we found 20 structural eigenmodes and 3 acoustic eigenmodes including one Helmholtz mode for the uncoupled system in the range of 0 to 500 Hz. Then, a coupled acoustic-structural analysis was performed. We found that the eigenfrequencies of the uncoupled systems were shifted only slightly after being coupled in the same frequency range. In Table 1, eigenfrequencies in the range of 0 to 500 Hz for uncoupled and coupled systems are listed for comparison.

Since we are only interested in the low frequency sound reduction, damping effect for the coupled acoustic-structural system was neglected. In the structural field, 1536 4-node plate elements are used and each of them is also treated as design variable for the stiffener design optimization formulation. In the acoustic field, 4096 8-node solid elements are constructed. To reduce the interior

**Table 1 Coupled and uncoupled eigenfrequencies of a 30 cm × 40 cm × 50 cm aluminum box**

Mode number	Structural frequency (Hz)	Acoustic frequency (Hz)	Coupled frequency (Hz)
1	-	0.00	0.00
2	114.95	-	117.02
3	130.72	-	129.92
4	179.50	-	178.67
5	195.32	-	194.99
6	195.36	-	196.09
7	231.06	-	239.07
8	242.49	-	241.66
9	257.62	-	254.44
10	291.94	-	291.35
11	302.71	-	302.71
12	323.13	-	304.21
13	335.41	-	330.40
14	-	344.05	370.61
15	387.39	-	382.70
16	389.28	-	386.75
17	411.79	-	411.72
18	418.62	-	418.62
19	-	430.06	443.02
20	443.03	-	443.33
21	462.87	-	452.73
22	484.05	-	482.94
23	494.91	-	495.40

sound level, the norm of acoustic excitation is chosen as design objective as we previously discussed. Four optimal design examples under different external excitations are presented below.

**5.1 Case 1.** In the first case, a unit harmonic excitation with frequency of  $\omega = 50$  Hz is applied at the center of the top plate as shown in Fig. 2. Using the proposed methodology, the norm of acoustic excitation is reduced from  $8.609643\text{e-}7$  to  $4.758937\text{e-}7$  in ten iterations and the overall interior sound decreased from 91.89 dB to 68.97 dB. The iteration history is showed in Fig. 3 and the trend of SPL reduction is listed in Table 2. The final stiffener configurations is shown in Fig. 4. It was found that the stiffener is mainly concentrated in the region where the external force applies, which is reasonable because the excitation frequency is lower than resonance frequencies of the system. The uncoupled structural frequencies and the coupled system frequencies in the range of 0 to 200 Hz are listed in Table 3. Comparing to the initial design with uniformly distributed stiffener material, we found that the final design also exhibits great changes of natural frequencies and mode shapes.

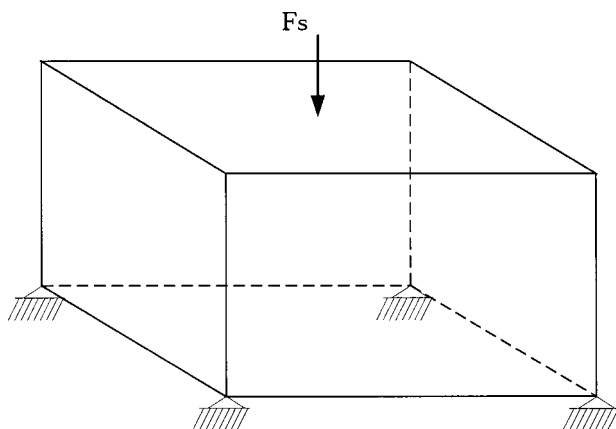


**Fig. 2 A box under an excitation loading at the center of the top plate**

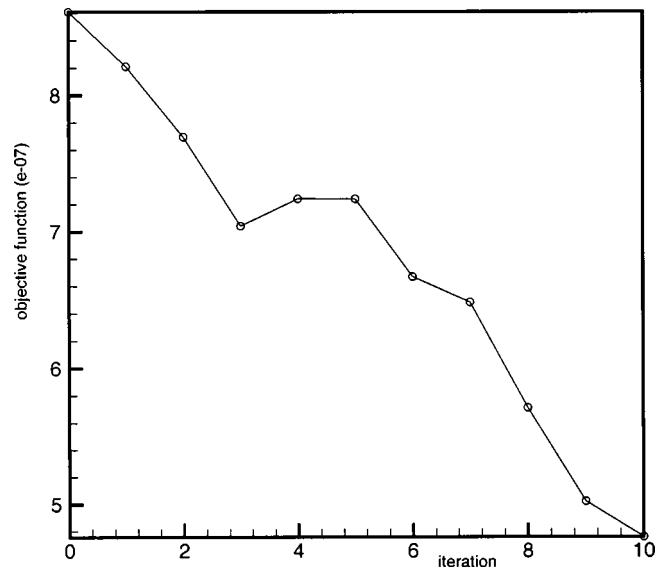


**Fig. 3 Iteration history of the objective function in case 1**

**5.2 Case 2.** In the second case, the unit harmonic excitation with the same excitation frequency as in the case 1 is applied to the center point of the flank plate as shown in Fig. 5.

Iteration history of the objective function is shown in Fig. 6 and we found the acoustic excitation is decreased from  $6.246733\text{e-}7$  to  $9.847646\text{e-}8$  with the overall interior sound level reduction from 76.73 dB to 51.92 dB in ten iterations. The result of the optimal stiffeners placement is shown in Fig. 7 and we can see the stiff-

**Table 2 Trend of interior SPL reduction in case 1**

Iteration number	Sound Pressure Level (dB)	Weight (Kg)
initial	91.89	5.5836
1	89.62	5.5836
2	80.87	5.5836
3	77.05	5.5836
4	75.64	5.5836
5	74.33	5.5836
6	72.08	5.5836
7	70.88	5.5836
8	70.52	5.5836
9	70.26	5.5836
10	68.97	5.5836

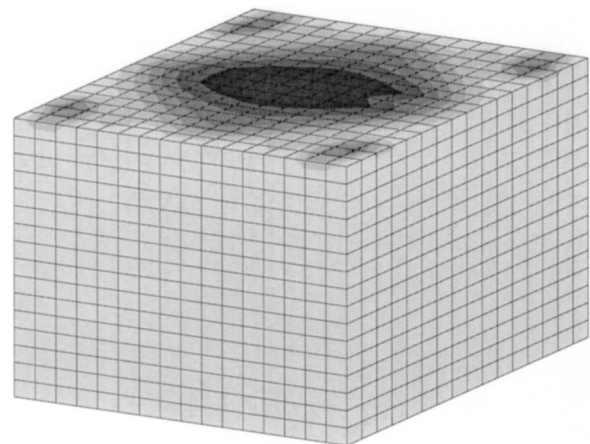


**Fig. 4 Optimal configuration of the stiffeners placement in case 1**

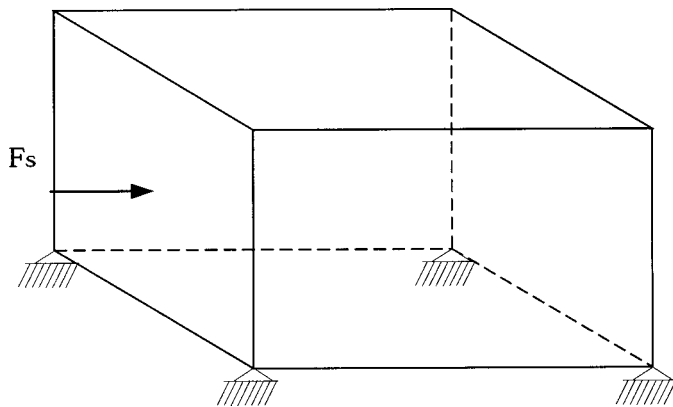
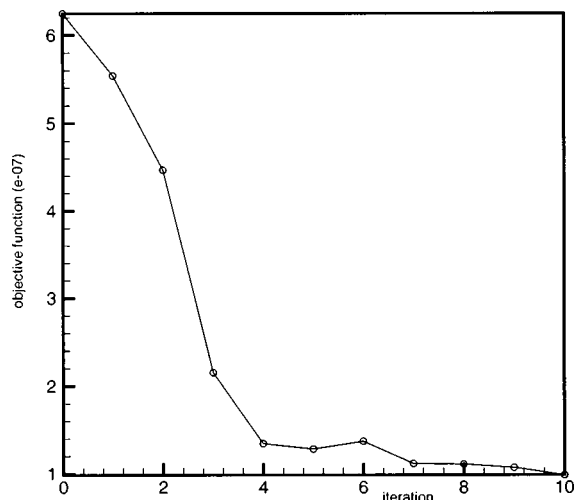
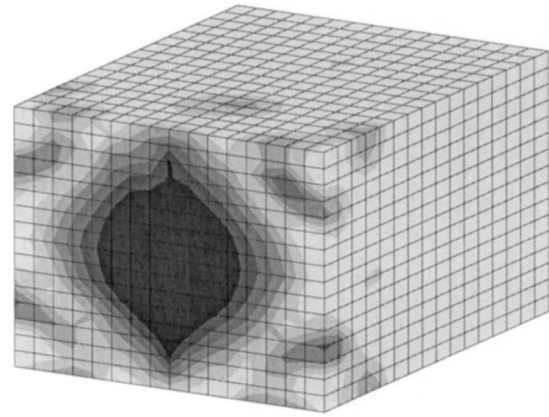


**Table 3 Natural frequencies of the final design in case 1**

Mode number	Structural frequency (Hz)	Coupled frequency (Hz)
1	-	0.00
2	70.18	72.31
3	120.74	120.27
4	120.87	120.53
5	124.97	125.10
6	138.17	146.12
7	147.54	148.25
8	177.84	177.51
9	185.15	184.02
10	190.37	187.38

eners are also mostly located in the external force applied region. Table 4 shows the trend of interior SPL reduction throughout the iterations. The corresponding uncoupled structural frequencies and coupled system frequencies in the range of 0 and 200 Hz are listed in Table 5. The final design also experiences changes in natural frequencies and mode shapes from the initial design.

**5.3 Case 3.** In the third case, a unit harmonic excitation with higher frequency is applied at the center of the top plate. The excitation frequency is chosen as  $\omega = 150$  Hz. We found the objective function reduced from  $2.811064e-5$  to  $1.548597e-5$  and the overall interior sound decreased from 80.13 dB to 67.03 dB after ten iterations. The iteration history is showed in Fig. 8 and the trend of SPL reduction is showed in Table 6. Fig. 9 shows the

**Fig. 5 A box under an excitation loading at the center of the flank plate****Fig. 6 Iteration history of the objective function in case 2****Fig. 7 Optimal configuration of the stiffeners placement in case 2**

optimal stiffener location. Unlike the first two cases, in this case the locations of stiffeners are spread out to different region of the box. This is due to the fact the excitation frequency is in the middle of several resonance frequencies of the system. To minimize the acoustic excitation, the add-on stiffeners try to reduce the effects from all these resonance modes as much as possible. The natural frequencies below 200 Hz of the final design are also listed in Table 7 for reference.

**5.4 Case 4.** In the last example, the stiffener design under a band of frequency excitation is studied. A unit harmonic excitation is applied at the center of the top plate with a band of low excitation frequencies ranged from 20 to 100 Hz. A modified objective function, Eq. (15), is used here. Since the excitation frequency range falls below any resonance frequency, the optimal stiffener location turns out to be very similar to that of the first case as Fig. 4. We found the objective function is reduced from  $3.106249e-7$  to  $1.842361e-7$  and the overall interior sound defined in Eq. (16) is decreased from 93.53 dB to 75.16 dB after ten iterations. Fig. 10 shows the interior SPL comparison between the initial design and the final design within the exciting frequency range.

**Table 4 Trend of SPL reduction in case 2**

Iteration number	Sound Pressure Level (dB)	Weight (Kg)
initial	76.73	5.5836
1	72.20	5.5836
2	61.03	5.5836
3	58.29	5.5836
4	57.33	5.5836
5	56.62	5.5836
6	56.90	5.5836
7	55.69	5.5836
8	53.92	5.5836
9	52.12	5.5836
10	51.92	5.5836

**Table 5 Natural frequencies of the final design in case 2**

Mode number	Structural frequency (Hz)	Coupled frequency (Hz)
1	-	0.00
2	104.94	107.27
3	117.86	117.13
4	158.14	157.36
5	167.27	167.43
6	188.17	195.37

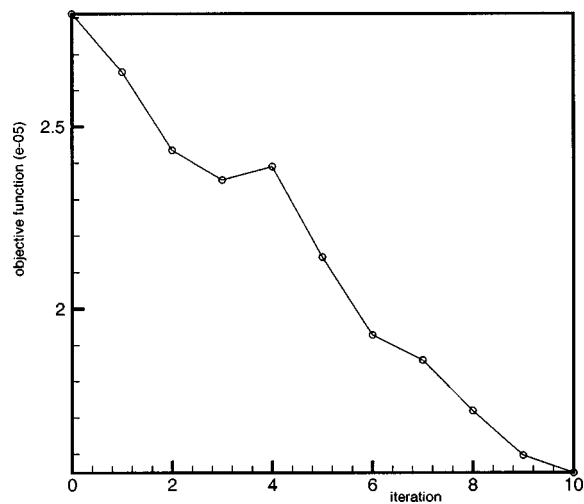


Fig. 8 Iteration history of the objective function in case 3

Table 6 Trend of interior SPL reduction in case 3

Iteration number	Sound Pressure Level (dB)	Weight (Kg)
initial	80.13	5.5836
1	79.59	5.5836
2	77.39	5.5836
3	74.91	5.5836
4	75.88	5.5836
5	73.40	5.5836
6	71.20	5.5836
7	70.46	5.5836
8	68.99	5.5836
9	67.63	5.5836
10	67.03	5.5836

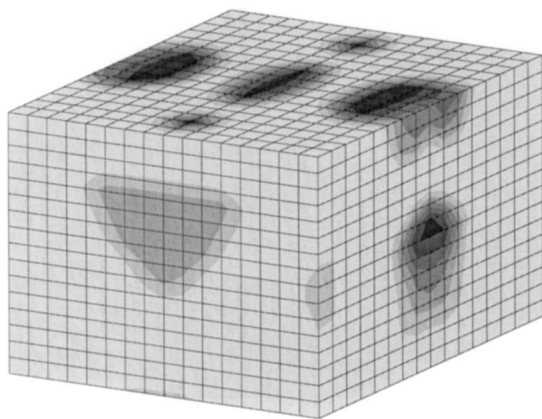


Fig. 9 Optimal configuration of the stiffeners placement in case 3

Table 7 Natural frequencies of the final design in case 3

Mode number	Structural frequency (Hz)	Coupled frequency (Hz)
1	-	0.00
2	88.77	90.39
3	115.09	115.62
4	161.26	160.88
5	166.55	166.00
6	173.40	173.79

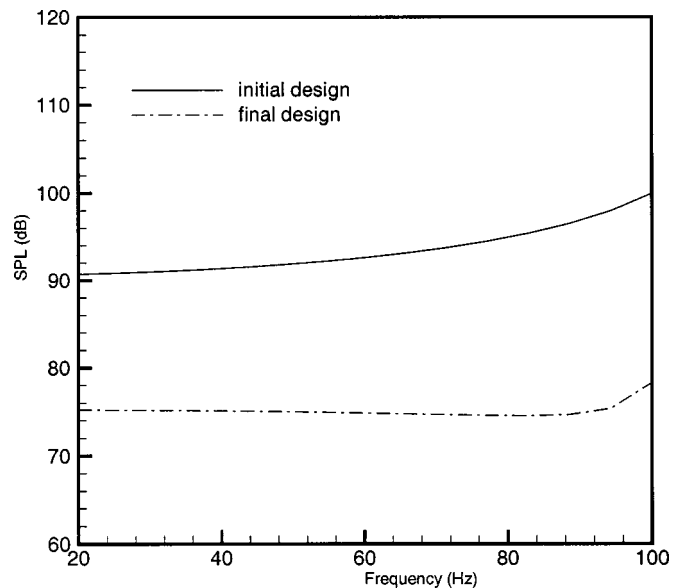


Fig. 10 Interior SPL comparison between the initial design and the final design

## 6 Conclusion and Future Work

In this paper, optimal stiffener design for interior sound reduction of coupled acoustic-structural system is studied. Forced frequency response and its sensitivity of this coupled system were solved by the modal analysis method. Using a topology optimization based approach, the optimal stiffener placement problem was converted into an optimal material distribution problem. Instead of using the overall interior sound level directly, the norm of acoustic excitation was used as the objective function and from our numerical examples, it showed the acoustic excitation is a good indicator for sound reduction. At low frequency excitations, the optimal stiffeners might be applied to the region near the external force source, however when the excitation frequency is among several resonance frequencies, stiffener might be placed throughout the structure in order to compensate the resonance modes involved. In this work, a conservative system with no damping effect is considered, therefore the proposed approach is only valid for single frequency excitation or a band of low frequency excitations without any resonance frequency included. More general method to handle damping is currently under investigation.

## References

- [1] Hagiwara, W., Kozukue, W., and Ma, Z. D., 1993, "The Development of Eigenmode Sensitivity Analysis Methods for Coupled Acoustic-Structural Systems and Their Application to Reduction of Vehicle Interior Noise," *Finite Elem. Anal. Design*, **14**, pp. 235–248.
- [2] Huff, J. E., Jr., and Bernhard, R. J., 1995, "Acoustic Shape Optimization Using Parametric Finite Elements," *ASME 1995 Design Engineering Technical Conferences*, DE-Vol. 84-2, pp. 577–584.
- [3] Wodtke, H. W., and Koopmann, G. H., 1995, "Quieting Plate Modes with Optimally sized Point Masses—A Volume Velocity Approach," *ASME 1995 Design Engineering Technical Conferences*, DE-Vol. 84-2, pp. 647–654.
- [4] Constans, E., and Belegundu, A., 1996, "Minimizing Radiated Sound Power from Vibrating Shells," *The 6th AIAA/NASA/ISSMO Symposium on Multidisciplinary Analysis and Optimization*, Bellevue, WA, Paper 96-4111, pp. 1106–1116.
- [5] Luo, J. H., and Gea, H. C., 1997, "Modal Sensitivity Analysis of Coupled Acoustic-Structural Systems," *J. Sound Vib.*, **119**, pp. 545–550.
- [6] Gea, H., 1996, "Topology Optimization: A New Micro-Structure Based Design Domain Method," *Comput. Struct.*, **61**(5), pp. 781–788.

- [7] Chickermane, H., and Gea, H. C., 1996, "A New Local Function Approximation Method for Structural Optimization Problems," *Int. J. Numer. Methods Eng.*, **39**, pp. 829–846.
- [8] Craggs, A., 1971, "The Transient Response of a Coupled Plate-Acoustic System Using Plate and Acoustic Finite Elements," *J. Sound Vib.*, **15**, pp. 509–528.
- [9] Diaz, A. R., and Kikuchi, N., 1992, "Solutions to Shape and Topology Eigenvalue Optimization Problems Using a Homogenization Method," *Int. J. Numer. Methods Eng.*, **35**, pp. 1487–1502.
- [10] Bendsøe, M. P., and Kikuchi, N., 1988, "Generating Optimal Topologies in Structural Design Using A Homogenization Method," *Comput. Methods Appl. Mech. Eng.*, **71**, pp. 197–224.